J|A|C|S COMMUNICATIONS

Published on Web 08/12/2009

Direct Observation of Millisecond to Second Motions in Proteins by Dipolar CODEX NMR Spectroscopy

Alexey Krushelnitsky,*,† Eduardo deAzevedo,‡ Rasmus Linser,§ Bernd Reif,§ Kay Saalwächter,*,|| and Detlef Reichert*,||

Kazan Institute of Biochemistry and Biophysics, Kazan, Russia, Instituto de Física de São Carlos, Universidade de São Paulo, São Carlos, Brazil, Leibniz-Institut für Molekulare Pharmakologie, Berlin, Germany, and Institut für Physik − NMR, Martin-Luther-Universität Halle-Wittenberg, Halle, Germany

Received May 13, 2009; E-mail: krushelnitsky@mail.knc.ru; kay.saalwaechter@physik.uni-halle.de; detlef.reichert@physik.uni-halle.de

The study of protein conformational dynamics is vitally important for the understanding of the molecular mechanisms underlying their biological function.[1] Internal motions on the microsecond to second time scale are of particular interest, since this is the time scale of many biologically relevant events, such as catalysis, recognition, folding, etc. In solution, the exact NMR assessment of such slow motions is challenged by the overall Brownian tumbling that averages dipolar, chemical shift anisotropy (CSA), and quadrupolar interactions. In contrast, in the solid state, these interactions can be beneficially employed to access the whole frequency range of internal protein dynamics, along with a direct elucidation of the geometric details of molecular motions. Studies of site-resolved internal dynamics in solid proteins to date have been limited to nanosecond to microsecond time scales.[2−5] For slower dynamics, there is still a considerable lack of experimental tools that can provide reliable quantitative information.

In this communication, we demonstrate for the first time a site-resolved study of slow (ms to s) motions in a microcrystalline protein, namely, the SH3 domain of α-spectrin. We apply an improved variant of a well-known solid-state magic-angle-spinning (MAS) exchange experiment, centerband-only detection of exchange (CODEX),[6] which yields direct time-domain dynamic information. CODEX was originally based on measuring changes in molecular orientation by means of changes in the CSA tensor orientation, which is encoded under MAS conditions by means of recoupling of π pulses in a way analogous to that in the well-known dipolar-recoupling rotational-echo double-resonance (REDOR) experiment.[7] CSA-based CODEX has previously been applied to the study of biomolecular dynamics,[6c] but it is subject to limitations that we improve upon herein.

We make use of the basic principle of CODEX, yet we employ heteronuclear dipolar couplings instead of CSA, which offers crucial advantages. In general terms, CODEX starts with an encoding during a time period A that under REDOR-type recoupling yields an accumulated phase ϕ_A. Magnetization is then stored along z during a mixing time τ_m, where molecular reorientation can occur. After τ_m, the magnetization is allowed to evolve during a period B under identical recoupling conditions, during which it accumulates a phase ϕ_B. When the pulse phases are properly set, the amplitude of the signal obtained after a readout period (another z storage followed by a readout pulse) is proportional to

$$I \sim \langle \cos \phi_A \cos \phi_B \rangle + \langle \sin \phi_A \sin \phi_B \rangle = \langle \cos(\phi_A - \phi_B) \rangle$$

where the brackets denote a powder average. If no change of molecular orientation occurs during τ_m, then $\phi_A = \phi_B$ and a full echo ($I_0 = 1$) is measured. If the tensor orientation is modulated by molecular motion, then $\phi_A \neq \phi_B$ and the signal intensity decreases. In the limit of long mixing and encoding times, the normalized intensity $I_\infty/I_0 = f_\infty = 1/N$ can be directly interpreted in terms of the number of sites N accessible to the process. The time scale of the original CODEX method is limited to the millisecond range at the lower end by the recoupling time itself,[8] and the upper limit in the second range is set by T_1 processes, (proton-driven) spin diffusion,[9] and T_1 relaxation processes of other nuclei (the relaxation-induced dipolar exchange with recoupling (RIDER) effect).[10]

Proton-driven spin diffusion among ^{15}N (not to mention ^{13}C) nuclei in fully enriched protonated proteins is in fact the major challenge for studying dynamics by means of solid-state exchange NMR, prompting us to apply CODEX to deuterated (proton-depleted) samples that were partially back-exchanged at labile sites.[11] Proton dilution provides not only suppression of spin diffusion but also a significant sensitivity enhancement in the case of indirect proton detection with high signal-to-noise ratio. Furthermore, the use of heteronuclear dipolar interactions instead of CSA is advantageous because XH dipolar tensors are usually larger than the CSA and have axial symmetry and orientations that are well-known from the structure. For this purpose, the REDOR train of π pulses is applied on the H channel (see Figure 1). The single

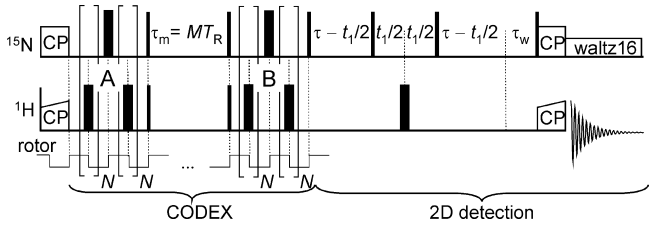

Figure 1. Dipolar CODEX pulse sequence. Thin and thick sticks denote $^{\pi}/_{2}$ and π pulses, respectively, and τ_w is a delay for better cancellation of the residual water signal.

X-channel π pulse in the middle of the encoding periods serves to remove the influence of isotropic chemical shifts. There must be an integer number of rotor periods before and after this π pulse; otherwise, part of the ^{15}N CSA and ^{2}H−^{15}N dipolar interactions would be reintroduced. Thus, the number of the rotor periods in the time intervals A and B must be an even number, and N (the number of ^{1}H π pulses within half of the periods A and B; see Figure 1) must be an odd number.

† Kazan Institute of Biochemistry and Biophysics.
‡ Universidade de São Paulo.
§ Leibniz-Institut für Molekulare Pharmakologie.
|| Martin-Luther-Universität Halle-Wittenberg.

For dipolar CODEX, the cos and sin components are related not just to the x and y components of the transverse X magnetization but to in-phase S_x and antiphase $2S_yI_z$ terms, respectively. As the most crucial advantage, couplings to other NMR-active nuclei, e.g., deuterons, are not reintroduced and thus do not pose problems related to their respective T_1 relaxation (RIDER). The unavoidable recoupling of dipolar interactions to other heteronuclei is one of the most serious limitations of the original CSA-based CODEX experiment.[10]

The antiphase term can create problems, as the I_z component is destroyed by spin exchange (actual exchange or spin diffusion) as well as faster T_1 relaxation.[10] In our sample, the ^{1}H T_1 was ~1.6 s, which would be a serious limitation. To avoid this, we reduced the original phase cycle so only the $\langle \cos \phi_A \cos \phi_B \rangle$ component related to in-phase magnetization was measured. This did not challenge the sensitivity of the experiment at all, as the sin counterpart would in any event be measured in separate transients as part of a longer phase cycle.[6] The experiment is thus largely similar to established stimulated-echo experiments that are very common in NMR analysis of static samples.[12] Notably, the sensitivity is reduced for passive spins with $I > {}^1/_2$ and for XH_n groups, for which the maximum amplitude of the cos−cos term is smaller.

We applied the experiment to ^{15}N−^{1}H dipolar pairs, but it can of course be applied to any other pair of magnetic nuclei. The pulse sequence in Figure 1 shows the combination of the dipolar CODEX part with a proton-detected ^{15}N−^{1}H 2D correlation experiment.[11] The use of a proton-depleted sample also provides longer effective T_2 relaxation times[13] (up to 100 ms) during the encoding delays and thus a better signal. By virtue of the restriction to encoding S_x in-phase magnetization, the experiment is not affected at all by fast interproton spin diffusion or relaxation, even in fully protonated samples. Proton-driven ^{15}N−^{15}N spin diffusion can also be ruled out, as previous work has demonstrated a spin-diffusion time scale of ~5 s in a fully protonated protein at 10 kHz MAS,[14] so the additional slowdown in the deuterated protein provides enough headspace.

An important experimental detail is the correction of the experimental CODEX exchange intensities (measured as a function of the mixing time τ_m) for T_1 relaxation of the observed ^{15}N nucleus. The original CODEX pulse sequence implements an internal T_1 normalization by means of referencing (dividing) the signal by that of a largely identical reference experiment with swapped mixing and z-filter delays.[6] This approach is elegant but has two drawbacks: first, the signal-to-noise ratio suffers as a result of the division by another noisy quantity, and second, the reference experiment sacrifices half of the spectral intensity because of separate z-storage of the cos and sin components during τ_m. We therefore correct for T_1 effects via a conventional separate measurement (as described in ref 5) and subsequent division of the exchange intensities by a (noiseless) spin−lattice relaxation decay function, as we did in our previous papers.[9,14]

Since there are also no losses due to T_2 relaxation, the T_1 measurements are ~4 times faster than the CODEX measurements, and the experimental uncertainties in the T_1 values (3−15%) do not challenge the results reported below. Most of the peaks showed single-exponential decays, but there were a few peaks that revealed double-exponential T_1 decays, which can be explained by (partial) overlap of signals, an example of which is discussed below. It should be noted that T_1 values that are comparable to the range of mixing times used in the CODEX experiment compromise the signal intensity at long mixing times, leading to larger error intervals at longer τ_m but not to large systematic errors. Details of the T_1 correction of the CODEX decays are illustrated in Figures S2 and S3 in the Supporting Information (SI).

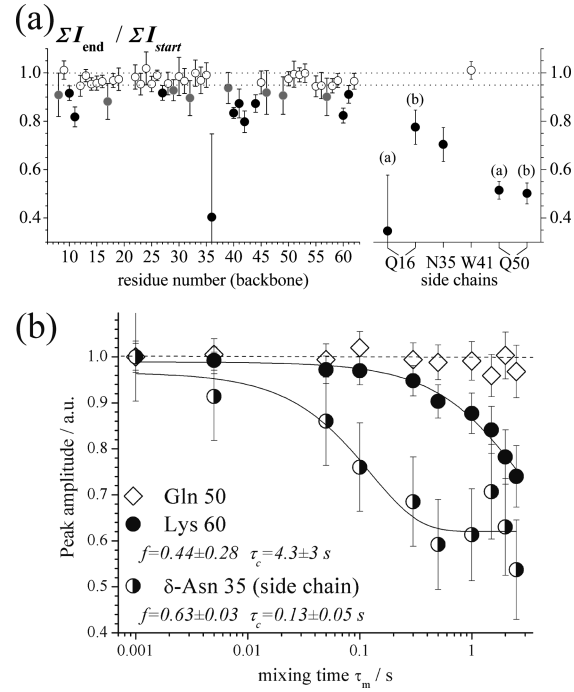

Figure 2. (a) Residue-resolved ratios of exchange intensities (corrected for spin−lattice relaxation) taken at the end (the last four points) and at the beginning (the first four points) of the CODEX decay, identifying residues with mobility on a ms-to-s scale. Solid circles define $\Sigma I_{end}/\Sigma I_{start}$ ratios with the upper limit of the error margin below 0.95. Gray circles define the ratios less than 0.95 for which the error margin exceeds the value of 0.95. (b) Examples of τ_m dependences for residues undergoing (Lys 60 and δ-Asn 35) and not undergoing (Gln 50) slow motions. The lines are exponential fits. Experimental conditions: Bruker Avance III 600 MHz spectrometer, narrow-bore 4 mm MAS probe, 10 kHz MAS at 14 °C, 0.8 ms encoding periods ($N = 7$; see Figure 1).

In Figure 2, we demonstrate the potential of the technique as applied to slow conformational motions in the SH3 domain of α-spectrin, which was perdeuterated with 20% back-substitution of labile protons. Ten mixing times between 1 ms and 2.5 s were recorded. To present the results of the analysis of the exchange decays for all of the peaks in one figure, we have plotted the ratio of the sum of the intensities of the last four points (1−2.5 s) of the decay to the sum of the intensities of the first four points (1 ms−0.1 s) of the same decay (see Figures S4 and S5 in the SI). This ratio provides a measure of the amplitude of the exchange decay with a relatively small experimental error and thus indicates residues undergoing slow motions. To identify signals undergoing exchange with appreciable amplitude beyond the experimental error, we have marked as black circles all the points in Figure 2a having an upper limit of the error margin less than 0.95. In addition, the remaining points in Figure 2a having an exchange ratio less than 0.95, regardless of their error, are marked in gray. The decays of all the marked peaks are shown in the SI. Thus, it is seen that about half the residues undergo slow motions. The large number of residues involved in slow motions is in fact expected, since infrequent large-scale conformational jumps in densely packed native proteins by default require correlated rearrangements of larger structural units. The color-coded presentation of mobile residues in the protein structure presented in Figure 3 shows that most of the residues undergoing slow motion are located at the termini and in a stretch in the center of the polypeptide chain from S36 to R49. It is important to mention that not only loops but also secondary-structure elements are involved in the slow motion.

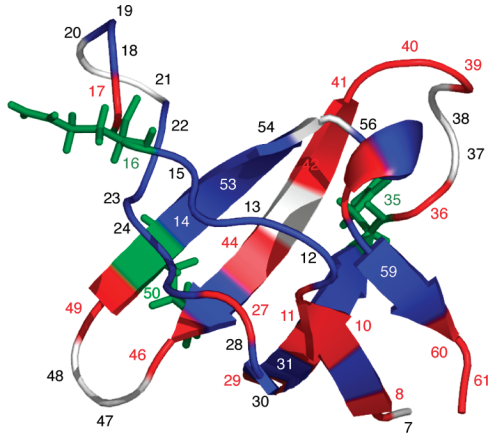

Figure 3. Structure of the α-spectrin SH3 domain with color-coded residue mobility: blue indicates immobile residues, and red (backbone) and green (side chains) indicate mobile residues (black and gray circles in Figure 2a). Residues that are unassigned or not seen in the spectrum are white.

Fitting of the decays with a single-exponential function, $I(\tau_m) \sim (1-f)\exp(-\tau_m/\tau_c) + f$ (see Figures 2b and S4) demonstrates that almost all the indicated residues feature correlation times of 1−3 s. Thus, it is likely that there is one dominant mode of slow motion in the protein involving a range of residues located in different parts of the spatial structure. There are only three exceptions that exhibit appreciably shorter correlation times: backbone peak Ser 36 and side-chain peaks Gln 16(b) and Asn 35 (see Figure S4 in the SI). However, Ser 36 has the largest experimental error of all the peaks, and thus, the fit of this decay is not very reliable. The fit of Gln 16(b) is problematic (see below), so the side chain of Asn 35 seems to be the only protein fragment undergoing another mode of slow motion independent of the rest of the molecule. However, this does not seem unreasonable for a separated side chain located on the protein surface.

It should be noted that the final plateau value f_∞ obtained at long mixing and encoding times might well be even lower than the plateau value that we observed in some cases, precluding for the moment the elucidation of geometric details of the motions, such as jump angles. Such work is time-consuming, as it requires checking the dependence on the recoupling time given in $N + 1$ rotor cycles (see Figure 1). Another challenge is that a potential preaveraging of the $^{15}N-^{1}H$ dipolar couplings resulting from faster motions on the picosecond to microsecond time scale must be quantified before the geometry can be addressed in any detail. Such investigations, using DIPSHIFT[15a] and Lee−Goldburg CP experiments,[15b] are underway. However, the fact that under the given conditions we have already observed long-time intensity values significantly less than 0.5 (and even values close to 0 for the side-chain signals) indicates that the corresponding residues undergo multisite jumps. We emphasize that the extracted correlation times are independent of the observed plateau values f and thus independent of the geometry of motion, at least in homogeneous systems without large-scale disorder, as is the case for our microcrystalline protein.

It is interesting to note that with only one exception (Trp 41), all the assigned side-chain signals (Gln 16, Asn 35, and Gln50) undergo slow motion. The exchange decays of the two side-chain nitrogens of ε-Gln 50 with $f \approx 0.2$ and $\tau_c \approx 1.7$ s are similar, as they should be, since conformational jumps experienced by this side chain must be equally reflected in the motion of two N−H bonds. The difference in the values of the f parameter for these two peaks (0.1 vs 0.3) is explained by the fact that the maximum mixing time used in the experiment was not long enough to reach the true plateau, resulting in a larger error in this parameter and a smaller systematic error in the correlation times (using longer mixing times would be of little help because of the relatively short T_1 of these peaks). At the same time, the τ_c of the two Gln 16 peaks (0.35 vs 2.5 s) are appreciably different, and this difference cannot be explained by uncertainty in the fits. The reason is the substantial overlap of the second peak (b) of ε-Gln 16 with another peak, namely, Val 23 of the backbone (see Figure S1 in the SI), which we did not attempt to deconvolute. The (static) contribution from Val 23 produces artificially high intensities at longer mixing times, leading to an apparently higher plateau and an unreliable fit. It should be noted that the T_1 correction fails in cases where the T_1's of superposed signals differ appreciably.

In summary, we have demonstrated the use a new dipolar exchange experiment for high-resolution biomolecular solid-state NMR spectroscopy that provides unique and as yet inaccessible *direct* (i.e., truly model-free) information on time scales and geometry of millisecond to second dynamics, paving the way for future applications in studies of actual protein function. In general, the presented data is free from interfering magnetic effects such as spin diffusion, RIDER, and T_1 relaxation, the latter only indirectly limiting the sensitivity of the method to measuring correlation times on the order of the ^{15}N T_1. Notably, observing slow motions on a second time scale in the liquid state by means of $R_2/R_{1\rho}$ dispersions[16] is problematic if not impossible. It is intriguing that even small, rigid globular proteins, such as the SH3 domain, show a rich variety of slow motions. Relating these motions to the dynamics of the protein in its native state (solution) is highly worthwhile, possibly elucidating internal constraints versus crystalline packing, and is a goal of future work.

Acknowledgment. This work was supported by the European Union (ERDF), the Fonds der Chemischen Industrie, and a grant from the Program "Molecular and Cell Biology" of the Russian Academy of Sciences. We thank V. Chevelkov and C. Hackel for their assistance in the experiments and data analysis.

Supporting Information Available: 2D spectrum with assignments, details of the T_1 correction of the CODEX decays, and examples of the CODEX mixing-time dependences for various peaks. This material is available free of charge via the Internet at http://pubs.acs.org.

References

(1) (a) Wand, A. J. *Nat. Struct. Biol.* **2001**, *8*, 926. (b) Karplus, M.; Kuriyan, J. *Proc. Natl. Acad. Sci. U.S.A.* **2005**, *102*, 6679.
(2) Giraud, N.; Bockmann, A.; Lesage, A.; Penin, F.; Blackledge, M.; Emsley, L. *J. Am. Chem. Soc.* **2004**, *126*, 11422.
(3) Hologne, M.; Faelber, K.; Diehl, A.; Reif, B. *J. Am. Chem. Soc.* **2005**, *127*, 11208.
(4) Lorieau, J. L.; McDermott, A. E. *J. Am. Chem. Soc.* **2006**, *128*, 11505.
(5) Chevelkov, V.; Diehl, A.; Reif, B. *J. Chem. Phys.* **2008**, *128*, 052316.
(6) (a) deAzevedo, E. R.; Hu, W.-G.; Bonagamba, T. J.; Schmidt-Rohr, K. *J. Am. Chem. Soc.* **1999**, *121*, 8411. (b) deAzevedo, E. R.; Hu, W.-G.; Bonagamba, T. J.; Schmidt-Rohr, K. *J. Chem. Phys.* **2000**, *112*, 8988. (c) deAzevedo, E. R.; Kennedy, S. B.; Hong, M. *Chem. Phys. Lett.* **2000**, *321*, 43.
(7) Gullion, T.; Schaefer, J. *J. Magn. Reson.* **1989**, *81*, 196.
(8) Saalwächter, K.; Fischbach, I. *J. Magn. Reson.* **2002**, *157*, 17.
(9) Krushelnitsky, A.; Reichert, D.; Hempel, G.; Fedotov, V.; Schneider, H.; Yagodina, L.; Schulga, A. *J. Magn. Reson.* **1999**, *138*, 244.
(10) Saalwächter, K.; Schmidt-Rohr, K. *J. Magn. Reson.* **2000**, *145*, 161.
(11) Chevelkov, V.; Rehbein, K.; Diehl, A.; Reif, B. *Angew. Chem., Int. Ed.* **2006**, *45*, 3878.
(12) Böhmer, R.; Diezemann, G.; Hinze, G.; Rössler, E. *Prog. NMR Spectrosc.* **2001**, *39*, 191.
(13) Chevelkov, V.; Reif, B. *Concepts Magn. Reson.* **2008**, *32A*, 143.
(14) Krushelnitsky, A.; Bräuniger, T.; Reichert, D. *J. Magn. Reson.* **2006**, *182*, 339.
(15) (a) deAzevedo, E. R.; Saalwächter, K.; Pascui, O.; de Souza, A. A.; Bonagamba, T. J.; Reichert, D. *J. Chem. Phys.* **2008**, *122*, 104505. (b) Cobo, M. F.; Maliňáková, K.; Reichert, D.; Saalwächter, K.; deAzevedo, E. R. *Phys. Chem. Chem. Phys.* **2009**, *11*, 7036.
(16) Palmer, A. G.; Kroenke, C. D.; Loria, J. P. *Methods Enzymol.* **2001**, *339*, 204.

JA9038888

Supporting Information for

Direct Observation of Millisecond to Second Motions in Proteins by Dipolar CODEX NMR Spectroscopy

Alexey Krushelnitsky*[1], Eduardo deAzevedo[2], Rasmus Linser[3], Bernd Reif[3], Kay Saalwächter*[4], Detlef Reichert*[4]

[1] *Kazan Institute of Biochemistry and Biophysics, Kazan, Russia;*
[2] *Instituto de Física de São Carlos, Universidade de São Paulo, São Carlos, Brazil;*
[3] *Leibniz-Institut für Molekulare Pharmakologie, Berlin, Germany;*
[4] *Institut für Physik – NMR, Martin-Luther-Universität Halle-Wittenberg, Halle, Germany.*

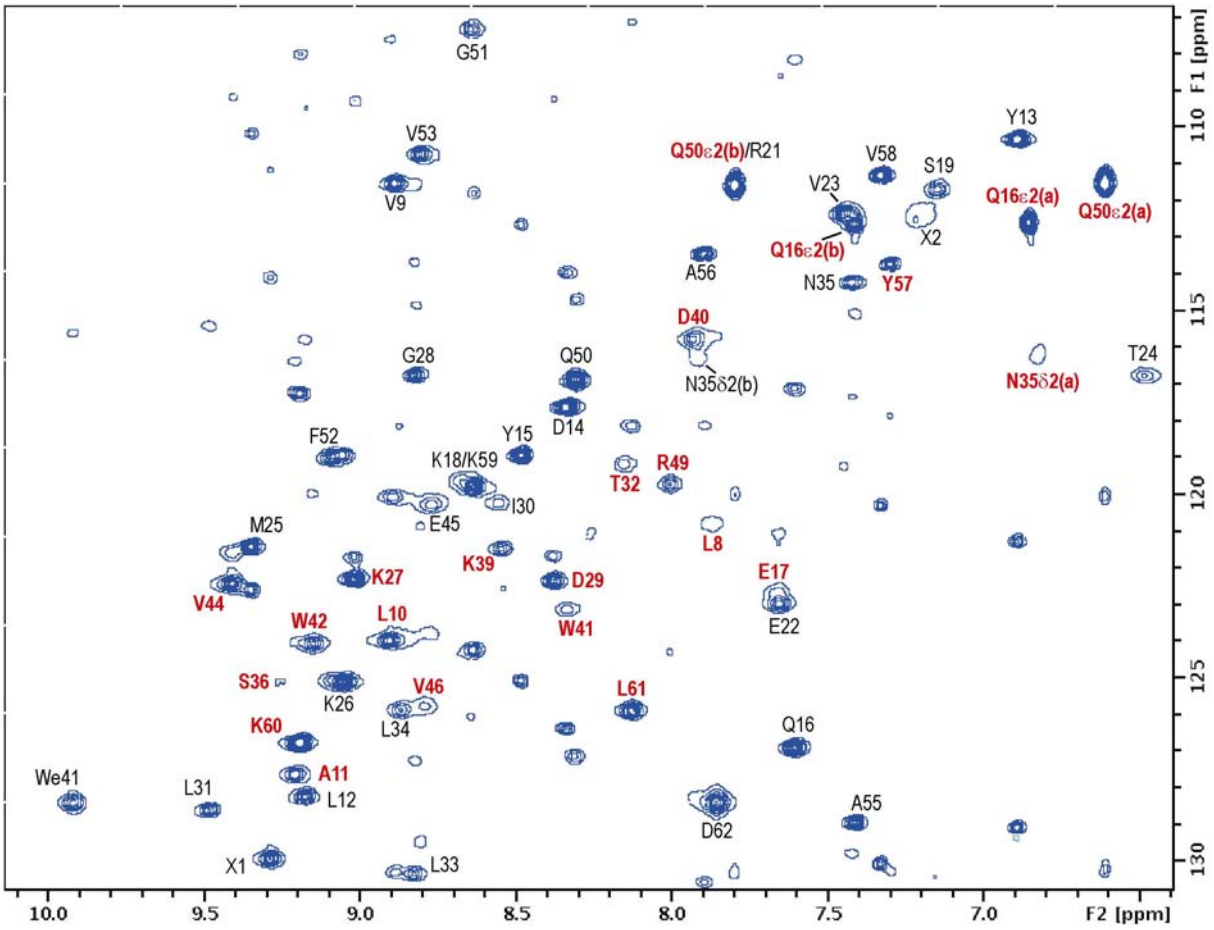

Figure S1. 2D proton detected ^{15}N-^{1}H correlation spectrum of the SH3-domain of α-spectrin, with assignment labels. All signals that have been observed to undergo slow exchange are marked in red (the decays of these peaks are shown in the Figures S4 and S5 below). Most of the unlabeled peaks in this spectrum are the spinning side bands that fold into the main spectrum area due to the narrow spectral width in the indirect (^{15}N) dimension. The second side chain peak of Q50 overlaps with the backbone R21 peak. However, the intensity of R21 is much lower than that of Q50 and thus can be neglected. The peak N35δ2(b) partially overlaps with D40 peak, it has much smaller intensity and thus the data for this peak could be determined reliably. X1 and X2 are two unassigned peaks. They do not undergo exchange and thus the data for these peaks are not shown in the paper.

The spectrum shown in Fig. S1 was obtained with the pulse sequence described in ref. 11. Experimental parameters: resonance frequency for protons 600 MHz, MAS rate 10 kHz, $T = 14$ ºC, repetition delay 2 s, indirect dimension spectral width 1550 Hz, indirect time domain 55 ms, number of scans 64. CODEX 2D exchange spectra were acquired using the same parameters, except for a higher number of scans (128). The acquisition of one CODEX 2D spectrum took from 11 h to one day depending on the mixing time (1 ms to 2.5 s). Side chain amide resonance assignments were obtained using standard HNCACB type experiments [R. Linser, U. Fink, B. Reif. *J. Magn. Reson.* 193 (2008) 89-93]. In this experiment, asparagines are readily assigned by identifying correlations from backbone and side chain amide proton resonances to resonances with identical Cα/Cβ chemical shifts. Similarly glutamines are assigned. Differentiation among different glutamine side chains relies uniquely on Cβ chemical shift dispersion.

Fig. S2 shows the details of the T_1-correction of the CODEX decays and ^{15}N spin-lattice relaxation rates ($R_1 = 1/T_1$) as a function of a residue number. In Fig. S3, we show examples for the fitting quality of the relaxation data, where the error intervals associated with R_1 are smaller than 10% in the shown cases (i.e., for residues for which T_1 is on the order of or not significantly longer than the typical slow-motion correlation time range). As can be seen on the right hand side, the uncertainty of the corrected CODEX data caused by R_1 uncertainty is much smaller than the internal experimental error of the CODEX experiment. Since the relaxation experiments were only conducted up to relaxation delays of 4 s, the error for those residues with very long T_1 (on the order of 10s and more) is larger, up to 15-25%. However, this long timescale is sufficiently separated from the timescale of the CODEX experiments, thus not introducing any substantial error.

In Fig. S4, exchange decays and fits are plotted for all peaks with the upper limit of the error margin below 0.95 in Fig. 2a (black circles). For comparison, Fig. S5 shows several noisier exchange decays for signals corresponding to the ratio values (regardless of the error bars) in Fig. 2a below 0.95 (grey circles).

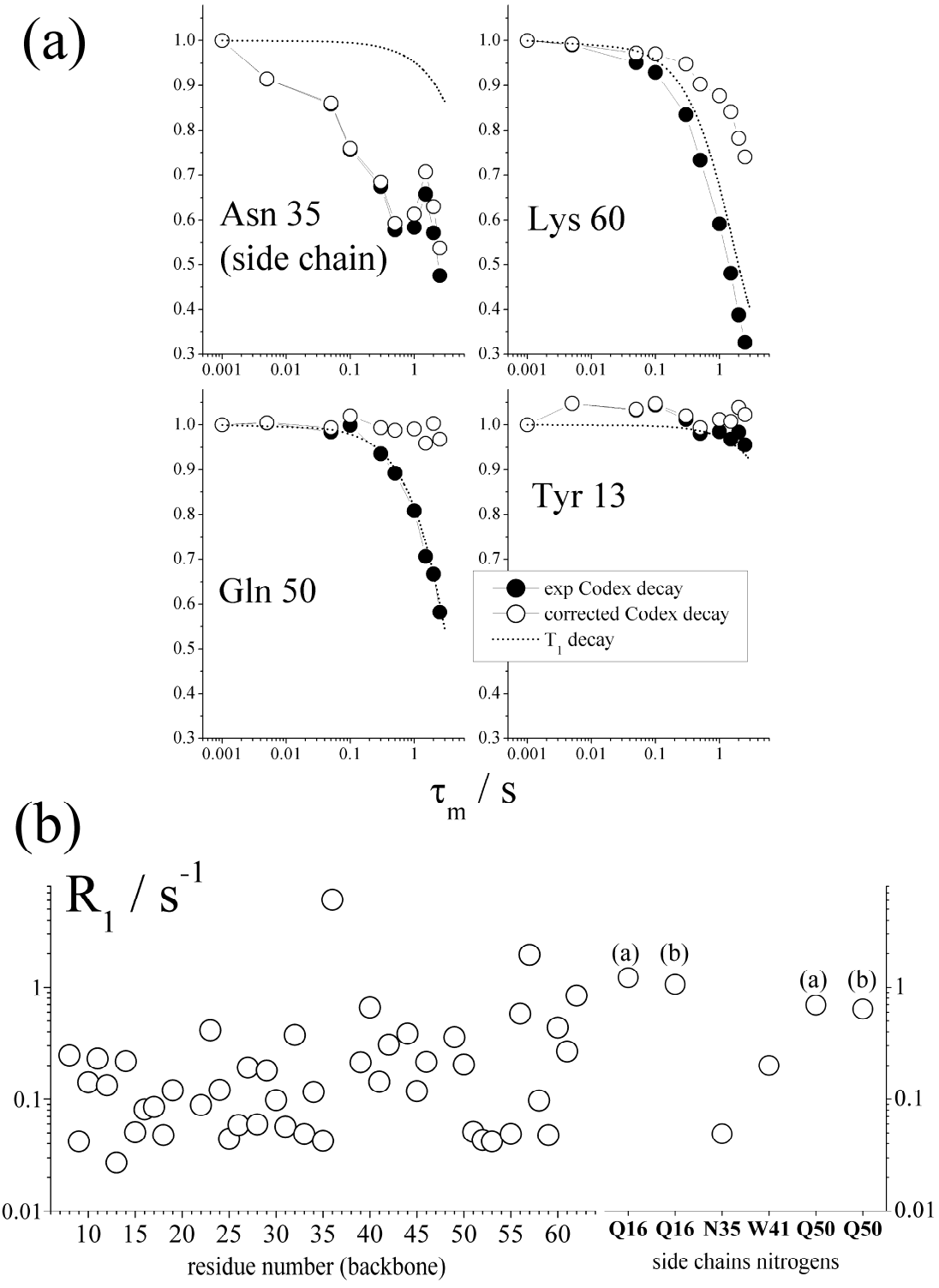

Figure S2. (a) Examples of raw (solid symbols) and corrected (open symbols) CODEX mixing time dependencies of peaks undergoing (top) and not undergoing (bottom) slow exchange. Dashed lines are the fits to spin-lattice relaxation data measured as described in ref. 5. The corrected data were obtained by dividing the peak intensity obtained in the CODEX experiment by spin-lattice relaxation decays:

$$I^*(\tau_m) = I(\tau_m)/\exp(-R_1\tau_m),$$

where $I^*(\tau_m)$ and $I(\tau_m)$ are the corrected and raw CODEX intensities, respectively; (b) ^{15}N spin-lattice relaxation rates $R_1=1/T_1$ as a function of residue number.

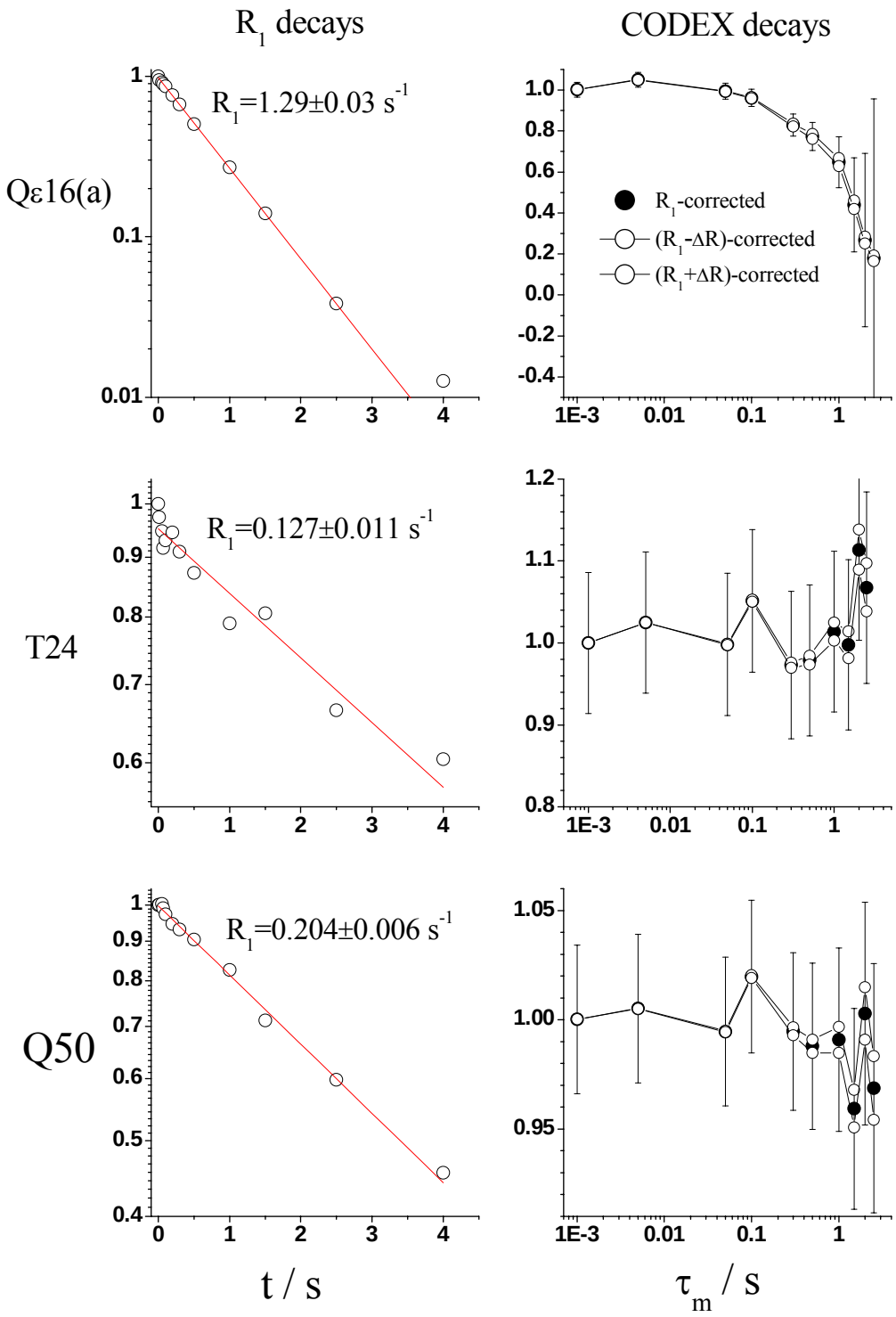

Figure S3. Examples demonstrating the fitting quality and the typical errors associated with the R_1 determination (left), and the robustness of the corrected CODEX data when using the fitted R_1 or the upper/lower ends of the error interval ($R_1 \pm \Delta R_1$) for correction (right). Red lines on the left are the exponential fits of the relaxation decays. Solid and (up and down) open circles on the right are the R_1-corrected CODEX decays corresponding to the average R_1 and ($R_1 \pm \Delta R_1$), respectively.

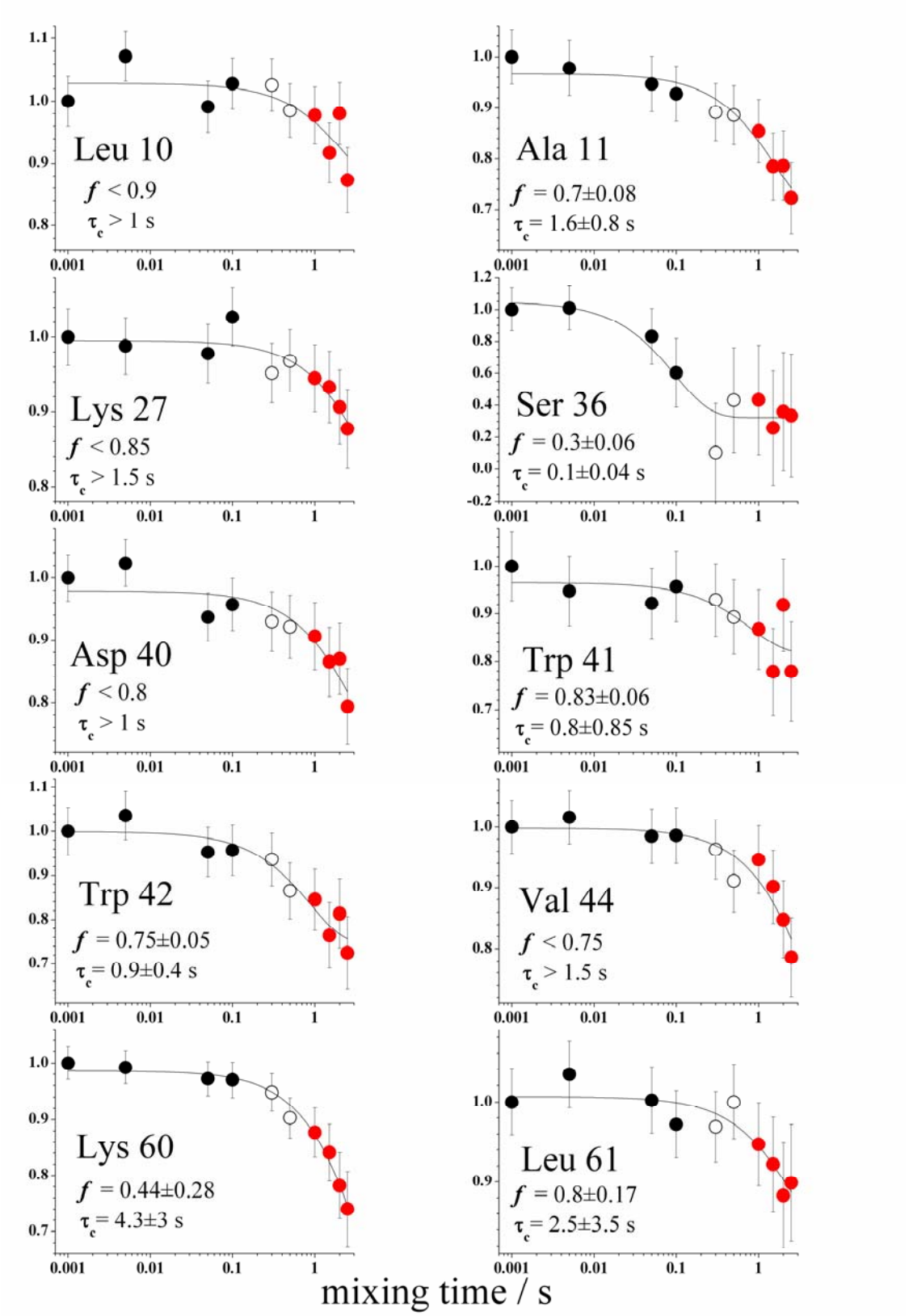

Figure S4 (a). T_1-corrected CODEX exchange decays and exponential fits according to $I(\tau_m) \sim f + (1-f)\cdot\exp(-\tau_m/\tau_c)$ for backbone signals that show exchange decay beyond experimental error (the upper limit of the error bar in Fig 2a is below 0.95, black circles). The solid symbols (black: short τ_m, red: long τ_m) denote the points which were averaged and used to calculate the ratio plotted in Fig. 2a of the paper. Because of the experimental error and relatively short range of τ_m, in some cases the fitting could only provide upper limits for f and lower limits for τ_c.

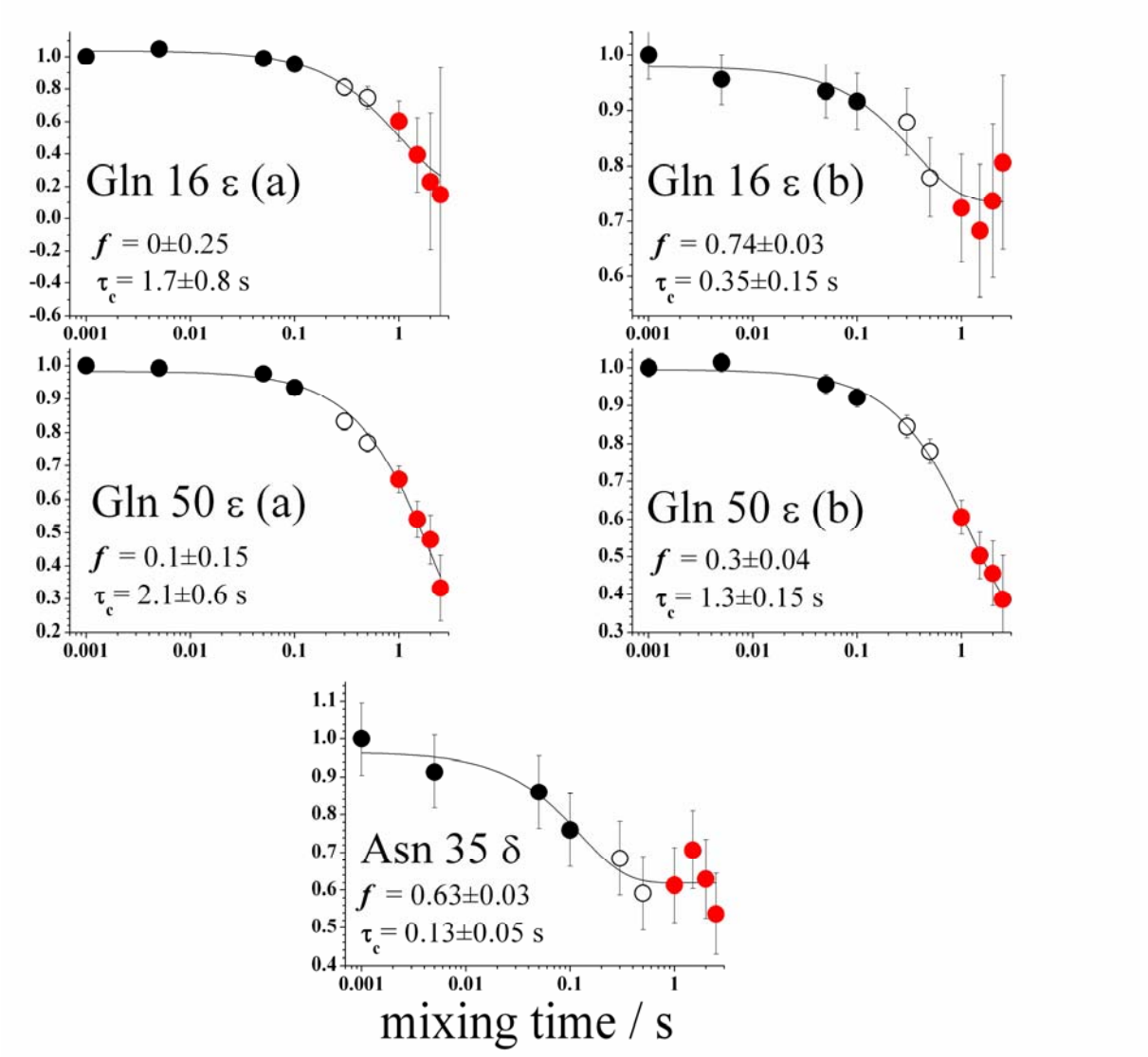

Figure S4 (b). Exchange decays and fits for the side chain peaks undergoing exchange beyond experimental error.

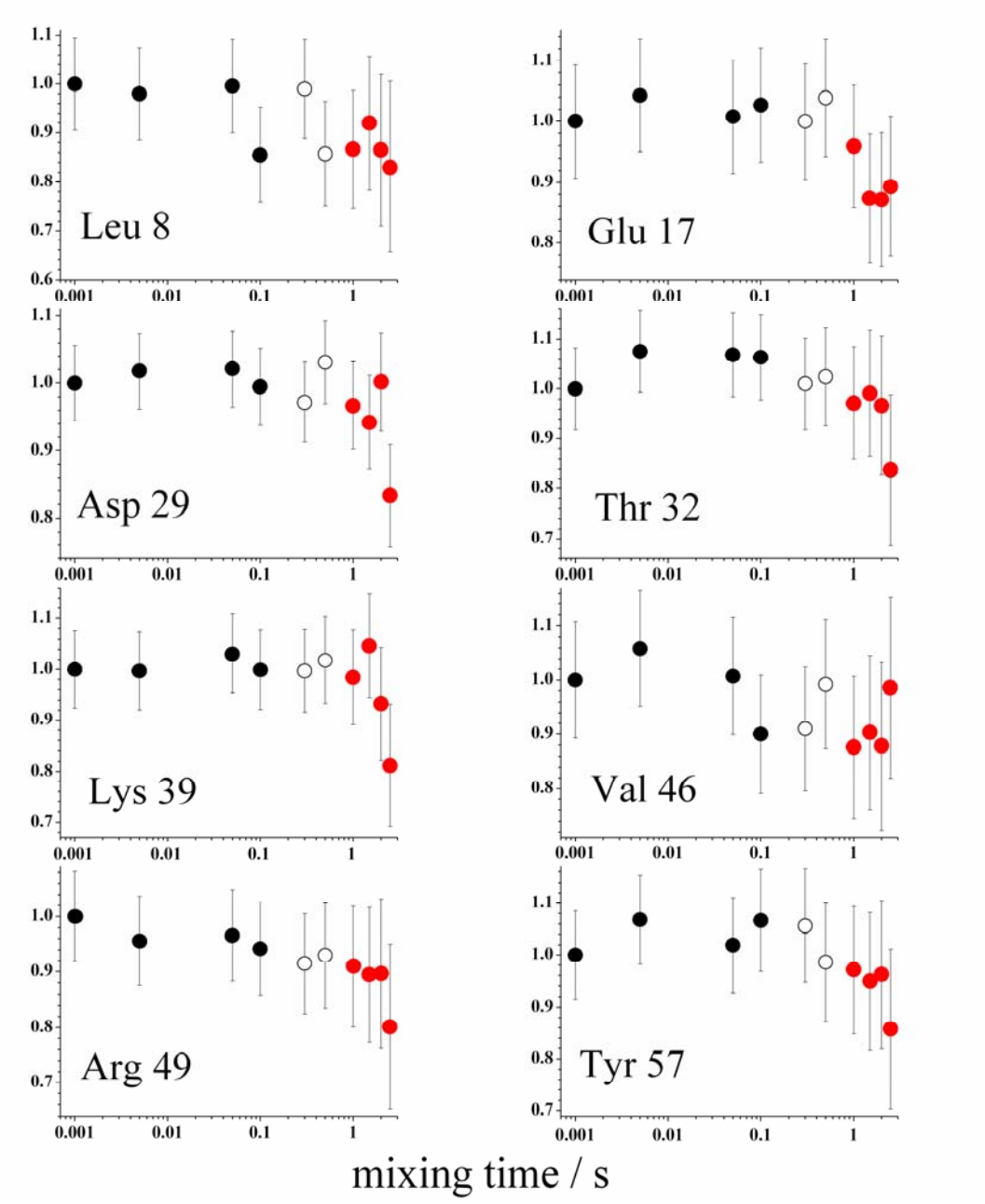

Figure S5. CODEX decays for the peaks corresponding to the intensities ratio below 0.95 in Fig 2a (grey circles). Because of the high experimental uncertainty, fitting of these data provides too ambiguous results and thus was not performed.